

B. P/T DETERMINATION

Because there is no thermal model computed for the study area, the temperature was determined using the formulas (B.1-B.3). The calculated temperature is a function of the surface and mantle heat-flow density or heat production (Q_s , Q_m , ρH_0 respectively), thermal conductivity k , and the thickness of the radiogenic upper-crustal layer h_r , for three different types of lithospheric geotherm over a certain depth z . The values of the heat-flow density are based on the estimates for the whole South American continent (Hamza&Muñoz, 1996; Muñoz, 1999). The surface heat-flow density values of the Patagonian Cordillera are characterized by high values ($>80\text{mW/m}^2$) while the Coastal Cordillera shows lower values ($<60\text{mW/m}^2$). For the continental case, the geotherms for two possible cases were examined. The first represents the colder forearc/and backarc regions while the second approximates the hotter volcanic arc case. For the colder situation, the heat-flow density value is 55mW/m^2 , with a corresponding mantle heat flow (B.4) of 30mW/m^2 . For the hotter volcanic arc area, surface heat flows of 70 and 100mW/m^2 were applied. The corresponding mantle heat flow for the warmer situation was calculated to be 56mW/m^2 . The mantle heat flow can be derived from the known surface heat flow, or vice-versa, using the following relationship (B.4)

The pressure was estimated following the formula B.5 as a function of the depth, standard density and overpressure factor. All the other parameters necessary for the temperature, and pressure estimation, were taken from Turcotte and Schubert (2002).

Conductive geotherm with crust heat generation using the surface heat flow “ Q_s ”

$$T(z) = \frac{Q_m}{k} z + \frac{(Q_s - Q_m)h_r}{k} (1 - e^{-z/h_r}) \quad (\text{B.1})$$

Conductive geotherm with crust heat generation using surface radiogenic heat production “ ρH_0 ”

$$T(z) = \frac{Q_m}{k} z + \frac{\rho H_0 h_r}{k} (1 - e^{-z/h_r}) \quad (\text{B.2})$$

Plate cooling model

$$T(z) = T_s + \frac{z}{2.32\sqrt{\kappa t}} (T_0 - T_1) + 0.1 \sin \frac{z\pi}{2.32\sqrt{\kappa t}} \quad (\text{B.3})$$

The following values of the constants were used to calculate the densities for the 3D modelling purposes (Turcotte & Schubert, 2002):

Q_s - surface heat flow density

Q_m - mantle heat flow density

for the cold and warm case respectively

k - thermal conductivity ($3\text{W m}^{-1}\text{ }^\circ\text{K}^{-1}$)

T_s - surface temperature ($25\text{ }^\circ\text{C}$)

h_r - thickness of the radiogenic layer (10 km)

ρH_0 - heat production (1.5mWm^{-3})

t - age of the oceanic lithosphere

κ - thermal diffusivity (mm^2/s)

$(T_0 - T_1)$ - temperature difference between the top and the bottom of the oceanic lithosphere

$$Q_m = Q_s - \rho H_0 h_r \quad (\text{B.4})$$

The pressure gradient is defined as:

$$P(z) = H * \rho * 9.8 * z \text{ where} \quad (\text{B.5})$$

H – overpressure factor

ρ – standard density (2.8 Mg/m³)

z- depth (in km)

The uncertainties associated with assigning densities arise not only from the complexity of the mineralogical reactions that occur within the subducted plate, but also from the lack of constraints and our poor knowledge of the thermal state of the working area. Some indications about the temperature structure come from the thermal model estimated for the Chilean subduction zone by Oleskevich et al. (1999) (Figure B.1). The two cross sections from Chile are comparable with thermal structure estimated for two cases (cold and warm subduction zone) in Japan. A predicted petrological model is presented in Figure B.2. The major difference between the profiles from Chile and Japan is the age of the two corresponding sections. The profiles for Chile are ~40 Ma and 100 Ma younger (for warm and cold situation respectively) relative to those estimated for Japan. These models can not be adopted in terms of the predicted thermal structure, composition and density values for the study area of this work, because they are models predicted for a specific subduction zone. The estimated thermal structure of the profiles for Japan is similar to the predicted profiles for Chile (Figure B.1), but only in terms of the assumed temperatures. In addition, both Chilean profiles are a few hundred kilometers away from the study area. Therefore, the results of this comparison were used in the modelling procedure only to give some preliminary ideas about possible compositions.

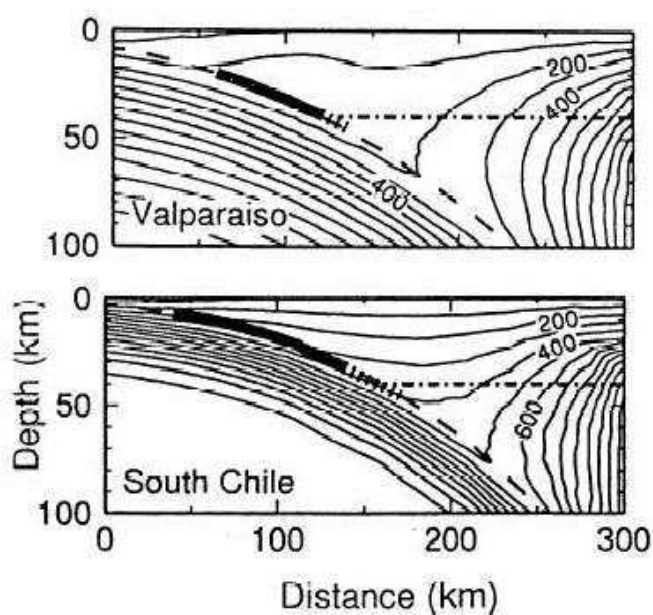


Figure B.1

The estimated thermal structure for a profile at Valparaíso (34°S) and south Chile (44°S) (Oleskevich, 1999). Distance is relative to the trench. The temperatures on the slab at a depth of 40 km reach ~350°C, whereas in the northern profile this temperature is reached at a much greater depth (below 70km).

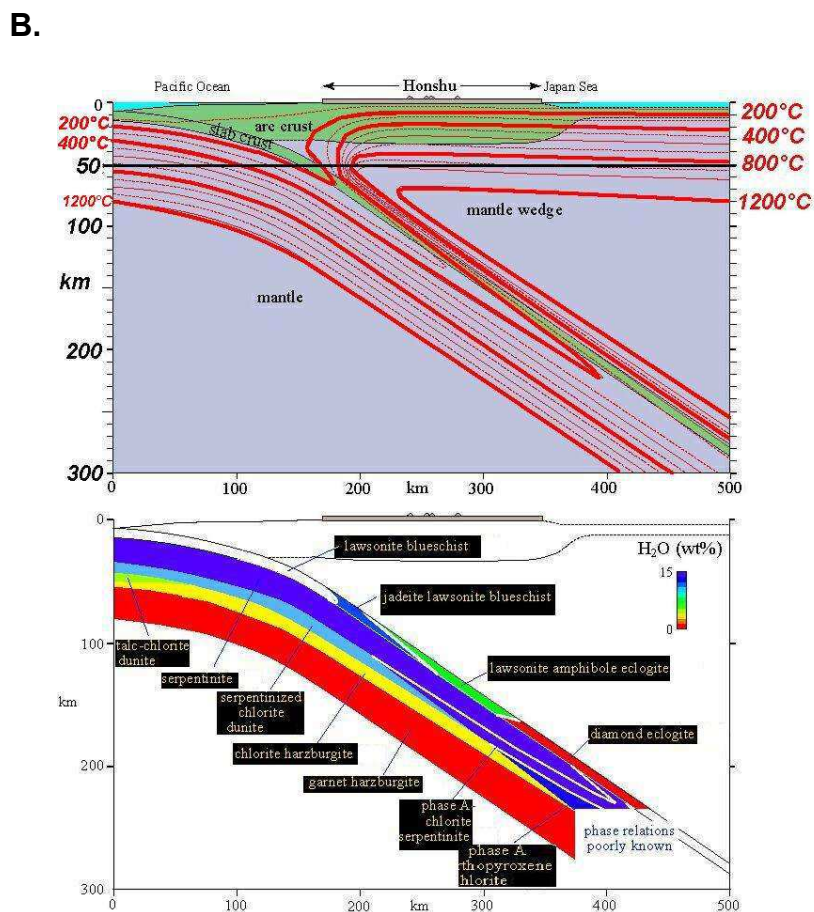
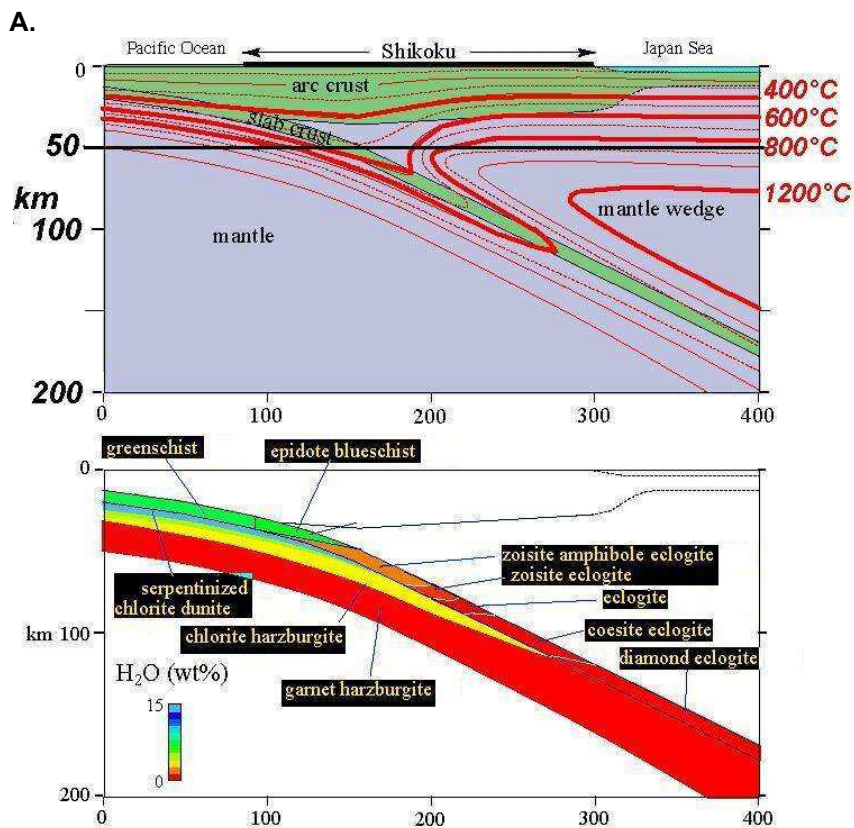


Figure B.2

The thermal and petrological model for the Nankai (A.) and Tohoku (B.) subduction zones showing a very warm thermal structure for the younger (45 Ma) oceanic plate (Nankai, SW Japan) compared to the old (130 Ma) and very cold subduction zone in northern Honshu. The lower parts of both figures show the estimated petrological model related to the computed thermal situation (Hacker et al. 2003).

